

# Bifurcation in ground-state fidelity for a one-dimensional spin model with competing two-spin and three-spin interactions

Hong-Lei Wang, Yan-Wei Dai, Bing-Quan Hu, and Huan-Qiang Zhou<sup>1</sup>

<sup>1</sup>*Centre for Modern Physics and Department of Physics,  
Chongqing University, Chongqing 400044, The People's Republic of China*

A one-dimensional quantum spin model with the competing two-spin and three-spin interactions is investigated in the context of a tensor network algorithm based on the infinite matrix product state representation. The algorithm is an adaptation of Vidal's infinite time-evolving block decimation algorithm to a translation-invariant one-dimensional lattice spin system involving three-spin interactions. The ground-state fidelity per lattice site is computed, and its bifurcation is unveiled, for a few selected values of the coupling constants. We succeed in identifying critical points and deriving local order parameters to characterize different phases in the conventional Ginzburg-Landau-Wilson paradigm.

PACS numbers: 03.67.-a, 03.65.Ud, 03.67.Hk

**Introduction.** Quantum phase transitions (QPTs) [1, 2], occurring at absolute zero temperature, are driven by quantum fluctuations in quantum many-body systems. In condensed matter, a theoretical description of such a system usually involves two-body interactions. However, recent progress makes it possible to realize multi-body interactions with current technology in experiments, which, as theoretical analyses unveiled, produce exotic quantum phases. Examples include a spin model with competing two-spin and three-spin interactions in a system of trapped ions [3] and of ultracold atoms in triangular lattices [4] and cold polar molecules [5]. Unfortunately, the presence of multi-body interactions in a spin model normally renders it not exactly solvable. This limits the applicability of conventional analytic approaches. Therefore, it is desirable to develop approximated techniques or fully numerical approaches to address such a novel many-body system.

In the past few years, significant progress has been made to develop efficient numerical algorithms to simulate quantum many-body lattice systems in the context of the tensor network representations [6, 7], resulting from advances in our understanding of quantum entanglement present in ground-state wave functions for quantum many-body lattice systems [8]. In Ref. [6], Vidal introduced the infinite time-evolving block decimation (iTEBD) algorithm to find an approximate ground state for an infinite-size one-dimensional (1D) lattice system in the infinite matrix product state (iMPS) representation. In Ref. [7], an infinite projected entangled-pair state (iPEPS) is proposed for an infinite-size quantum system in two and higher spatial dimensions. A peculiar feature of these algorithms is their ability to compute the ground-state fidelity per lattice site [9]- [13]. Fidelity describes the distance between two given quantum states, thus enabling us to capture drastic changes in ground-state wave functions for quantum many-body lattice systems undergoing QPTs [9]- [22]. In Refs. [9, 10], it was argued that the ground-state fidelity per lattice site is able to characterize QPTs, regardless of what type of internal order is present in quantum many-body states underlying various quantum lattice systems in condensed matter. However, an adaptation of the algorithms is necessary to make it possible to investigate a spin model with multi-body

interactions.

In this work, we first adapt the iTEBD algorithm, making it suitable to generate a ground-state wave function for a 1D translation-invariant spin model with the competing two-body and three-body interactions in the context of the iMPS representation. Then the ground-state fidelity per lattice site is computed, and its bifurcations is unveiled for different values of the truncation dimension, with a bifurcation point as a pseudo-critical point, which tends to the critical point when the truncation is removed. In addition, the bifurcation implies symmetry spontaneous breaking, characterized by a local order parameter, a central concept in the conventional Landau-Ginzburg-Wilson paradigm [23, 24]. The latter is read off from a reduced density matrix of a representative ground-state wave function from a given phase.

*Infinite matrix product state algorithm adapted to a spin model with three-body interactions.* We first describe an iMPS algorithm adapted to a spin model with three-body interactions. For an infinite-size translation-invariant quantum many-body system with three-body interactions described by a Hamiltonian  $H = \sum_i h^{[i,i+1,i+2]}$ , we introduce the iMPS representation that is translation-invariant under a three-site shift. That means we need three three-index tensors  $\Gamma_{Alr}^i$ ,  $\Gamma_{Blr}^j$ , and  $\Gamma_{Clr}^k$  and three diagonal matrices  $\lambda_A$ ,  $\lambda_B$ , and  $\lambda_C$  to store a wave function in the context of the iMPS representation, as shown in Fig. 1(i). Here,  $i, j$ , and  $k$  are physical indices, which run over a  $d$ -dimensional local Hilbert space,  $l$  and  $r$  are the inner bond indices,  $l, r = 1, \dots, \chi$ , with  $\chi$  being the truncation dimension. This amounts to the statement that the unit cell of the iMPS representation consists of three consecutive sites. The ground-state wave function is projected out by resorting to the imaginary time evolution.

The updating procedure of the algorithm is as follows. Apply a three-site imaginary time evolution gate  $U(i, i+1, i+2) = \exp(-h^{[i,i+1,i+2]}\Delta\tau)$  over a time slice,  $\Delta\tau \ll 1$ , to the unit cell of the iMPS representation, and contract all the tensors, as shown in Fig. 1(i). As such, we have a tensor  $M_{ABC}$  (Fig. 1(ii)). Reshape the tensor  $M_{ABC}$  into a  $\chi d^2 \times \chi d$  matrix and perform the singular value decomposition (SVD) to the matrix, we get  $M_{AB}$ ,  $\tilde{\lambda}_C$ , and  $M_C$ , as shown in Fig. 1(iii). Contract the tensor

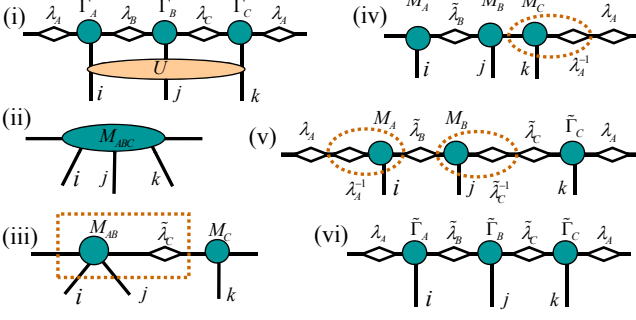


FIG. 1: (color online) The updating steps of an infinite matrix product state (iMPS) algorithm adapted to a spin model with three-body interactions. Here,  $\Gamma_\eta$  and  $\lambda_\eta$  ( $\eta = A, B, C$ ) are three-index tensors and diagonal matrices, respectively. (i) Apply a three-site gate  $U_{i,j,k}$  to the cell. (ii) Contract all the tensors in (i) and reshape the tensor  $M_{ABC}$  into a matrix. (iii) Perform the singular value decomposition (SVD) to yield  $M_{AB}$ ,  $\tilde{\lambda}_C$ , and  $M_C$ . (iii) Contract the tensor  $M_{AB}$  and  $\tilde{\lambda}_C$  and reshape it into a matrix. (iv) Perform the SVD to yield  $M_A$ ,  $\tilde{\lambda}_B$ , and  $M_B$ . (v) Restore the iMPS representation with the identity resolution  $\lambda_\eta \lambda_\eta^{-1} = \text{id}$  inserted. (vi) The diagonal matrices  $\tilde{\lambda}_B$ ,  $\tilde{\lambda}_C$ , and tensors  $\tilde{\Gamma}_A$ ,  $\tilde{\Gamma}_B$ , and  $\tilde{\Gamma}_C$  are updated, as indicated by the dash-line ovals in (iv) and (v).

$M_{AB}$  and  $\tilde{\lambda}_C$  and reshape it into a  $\chi d \times \chi d$  matrix and perform the SVD, we have  $M_A$ ,  $\tilde{\lambda}_B$ , and  $M_B$ , as seen in Fig. 1 (iv). Insert the identity resolution  $\lambda_A \lambda_A^{-1} = \text{id}$  and contract  $M_C$  and  $\lambda_A^{-1}$  to yield  $\tilde{\Gamma}_C$ . In Fig. 1 (v), the identity resolution  $\lambda_\eta \lambda_\eta^{-1} = \text{id}$  ( $\eta = A$  and  $C$ ) is inserted, thus we are able to update the diagonal matrices  $\tilde{\lambda}_B$ ,  $\tilde{\lambda}_C$ , and tensors  $\tilde{\Gamma}_A$ ,  $\tilde{\Gamma}_B$ , and  $\tilde{\Gamma}_C$ . Once this is done, we shift one site, apply the gate  $U(i+1, i+2, i+3)$ , and repeat the updating procedure. Afterwards, shift one site, apply the gate  $U(i+2, i+3, i+4)$  and repeat the updating procedure again. This completes our updating procedure for a time slice  $\Delta\tau$ . Iterating until the ground-state energy is converged, the system's ground-state wave function is yielded in the iMPS representation.

**Model.** We consider a 1D spin model with the competing two-spin and three-spin interactions [3], which is described by the Hamiltonian:

$$H = J_2 \sum_i \sigma_z^{[i]} \sigma_z^{[i+1]} + J_3 \sum_i \sigma_z^{[i]} \sigma_z^{[i+1]} \sigma_z^{[i+2]} - h \sum_i \sigma_x^{[i]}, \quad (1)$$

where  $J_2$  and  $J_3$  are, respectively, the two-spin and three-spin coupling constants,  $h$  is an external field along the  $x$  direction, and  $\sigma_\alpha^{[i]}$  ( $\alpha = x, z$ ) are the spin 1/2 Pauli operators at the  $i$ -th site. If the coupling constants are varied independently, it undergoes QPTs, with the occurrence of different quantum phases: an antiferromagnetic (AF) phase, a ferrimagnetic (F) phase, and a disordered paramagnetic (P) regime where spins are aligned along the  $x$  direction [3]. Note that, if  $J_3 = 0$ , the model Hamiltonian  $H$  becomes quantum Ising model in a transverse field, which is exactly solvable, with the critical point at  $h/J_2 = 1$ . A schematic phase diagram [3] is shown in Fig. 2. Here, we fix  $h=1$  and focus on three cases: (i)  $J_2=0.4$ ,

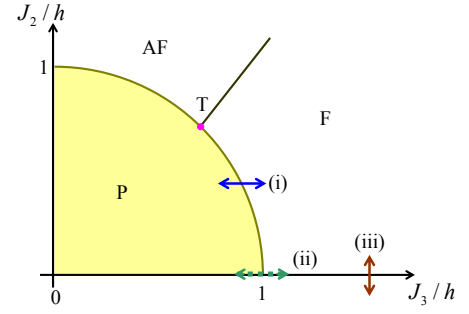


FIG. 2: (color online) Schematic phase diagram for a 1D spin model with the competing two-spin and three-spin interactions. For  $J_2 > 0$  and  $J_3 > 0$ , there are three phases: a disordered paramagnetic (P) regime, an antiferromagnetic (AF) order phase, and a ferrimagnetic (F) phase. Three phases coexist in the tricritical point T. In addition, the model becomes quantum Ising chain in a transverse field if  $J_3 = 0$ . We focus on three typical cases: (i) The horizontal double arrow crosses the phase boundary from P to F along  $J_2/h=0.4$ . (ii) The horizontal dotted double arrow crosses a critical point along  $J_2/h=0$ . (iii) The vertical double arrow crosses a discontinuous QPT point along  $J_3/h=1.5$ .

$J_3$  varies from  $J_3 = 0.80$  to  $J_3 = 1.00$  (horizontal solid double arrow in Fig. 2). (ii)  $J_2=0$ ,  $J_3$  varies from  $J_3 = 0.90$  to  $J_3 = 1.10$  (horizontal dotted double arrow in Fig. 2). (iii)  $J_3=1.5$ ,  $J_2$  varies from  $J_2 = -0.1$  to  $J_2 = 0.1$  (vertical solid double arrow in Fig. 2).

**Bifurcation in the ground-state fidelity per lattice site and symmetry spontaneous breaking.** For two ground-state wave functions  $|\varphi(\lambda_1)\rangle$  and  $|\varphi(\lambda_2)\rangle$ , with  $\lambda_1$  and  $\lambda_2$  being two values of the control parameter  $\lambda$ , the ground-state fidelity  $F(\lambda_1, \lambda_2) = |\langle \varphi(\lambda_1) | \varphi(\lambda_2) \rangle|$  asymptotically scales as  $F(\lambda_1, \lambda_2) \sim d(\lambda_1, \lambda_2)^L$ , where  $L$  is the number of the lattice sites. The scaling parameter,  $d(\lambda_1, \lambda_2)$ , first introduced in Ref. [9], characterizes how fast the ground-state fidelity goes to zero when the thermodynamic limit is approached. Physically,  $d(\lambda_1, \lambda_2)$  is the *averaged* ground-state fidelity per lattice site,

$$\ln d(\lambda_1, \lambda_2) = \lim_{L \rightarrow \infty} \frac{F(\lambda_1, \lambda_2)}{L}. \quad (2)$$

As discussed in Refs. [9, 10], it is well defined in the thermodynamic limit, although  $F(\lambda_1, \lambda_2)$  becomes trivially zero. The ground-state fidelity per lattice site is able to locate a QPT in a quantum many-body lattice system, regardless of what type of internal order is present.

The iMPS representation allows to efficiently compute the ground-state fidelity per lattice site [10]. Now we turn to the simulation results for the three cases, as selected above, of the model Hamiltonian (1) in the context of the iMPS algorithm.

(i)  $J_2 = 0.4$  and  $h = 1$ , and  $J_3$  is chosen as the control parameter. The ground-state fidelity per lattice site is plotted in Fig. 3(a), with the truncation dimension  $\chi = 8, 16$ , and 32, respectively. Note that,  $|\varphi(J'_3)\rangle$ , with  $J'_3 = 1.00$ , is chosen as a reference state. We observe that there is a bifurcation point

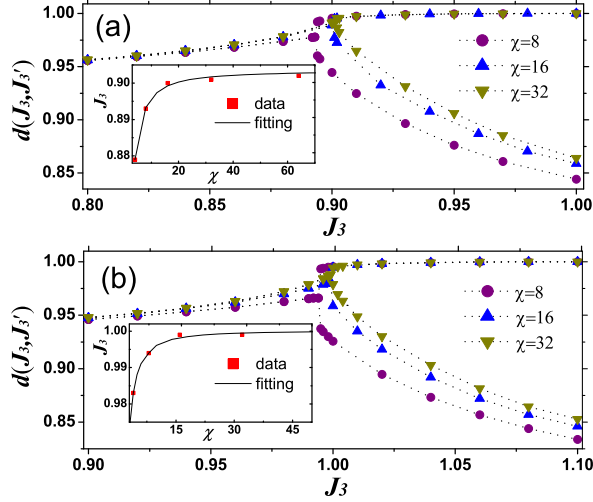


FIG. 3: (color online) Main: The ground-state fidelity per lattice site,  $d(J_3, J'_3)$ , as a function of  $J_3$ , at a fixed  $J'_3$ , for a 1D spin model with the competing two-spin and three-spin interactions. Here,  $J_2 = 0.4$  (a) and  $J_2 = 0$  (b), respectively, and  $J_3$  is chosen as the control parameter. In addition,  $|\varphi(J'_3)\rangle$ , with  $J'_3 = 1.00$  and  $J'_3 = 1.10$ , is chosen as a reference state, respectively, in (a) and (b). We observe that there is a bifurcation point in the ground-state fidelity per lattice site, indicating that spontaneous symmetry breaking occurs when the control parameter  $J_3$  varies. The bifurcation point is a pseudo critical point for a given value of the bond dimension. Inset: An extrapolation with respect to the bond dimension is performed for the pseudo critical points for  $\chi=4, 8, 16, 32$ , and  $64$ , yielding the critical points  $J_{3c} \sim 0.9034$  (a) and  $J_3 \sim 1.0001$  (b), when  $\chi \rightarrow \infty$ .

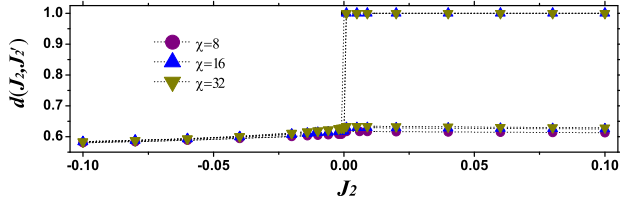


FIG. 4: (color online) The ground-state fidelity per lattice site,  $d(J_2, J'_2)$ , as a function of  $J_2$ , at a fixed  $J'_2$ , for a 1D spin model with the competing two-spin and three-spin interactions. Here,  $J_3 = 1.5$ , and  $J_2$  is chosen as the control parameter. In addition, the reference state  $|\varphi(J'_2)\rangle$  is fixed at  $J'_2 = 0.10$ . Spontaneous symmetry breaking occurs with  $J_2 > 0$ . A jump occurs in the ground-state fidelity per lattice site, meaning that the phase transition is discontinuous. The pseudo critical points are shown for different values of the truncation dimension, without any significant shift from  $\chi = 8$  to  $\chi = 32$ .

in the ground-state fidelity per lattice site, arising from spontaneous symmetry breaking of the  $Z_3$  translational invariance under three-site shifts, when the control parameter  $J_3$  varies from  $J_3 = 0.80$  to  $J_3 = 1.00$ . The bifurcation point is a pseudo critical point for a given value of the truncation dimension. The extrapolation of the pseudo critical points for  $\chi=4, 8, 16, 32$ , and  $64$  yields the critical point  $J_{3c} = 0.9034$ , when

$\chi \rightarrow \infty$ . Therefore, a continuous QPT occurs at  $J_{3c} \sim 0.9034$ .

(ii)  $J_2 = 0$  and  $h = 1$ , and  $J_3$  is chosen as the control parameter. The ground-state fidelity per lattice site,  $d(J_3, J'_3)$ , as a function of  $J_3$ , at a fixed  $J'_3$ , is plotted in Fig. 3(b), with the truncation dimension  $\chi = 8, 16$ , and  $32$ , respectively. The reference state  $|\varphi(J'_3)\rangle$  is chosen at  $J'_3 = 1.10$ . We observe that there is a bifurcation point in the ground-state fidelity per lattice site. Actually, four degenerate ground states arise from spontaneous symmetry breaking of the group  $G = Z_2 \times Z_2 \times Z_2/Z_2$ , when the control parameter  $J_3$  varies from  $J_3 = 0.90$  to  $J_3 = 1.10$ . Here, four  $Z_2$  groups are, respectively, generated from  $\sigma_z^A \sigma_z^B, \sigma_z^B \sigma_z^C, \sigma_z^A \sigma_z^C$ , and  $\sigma_z^A \sigma_z^B \sigma_z^C$ , where  $A, B$ , and  $C$  label three sites in the unit cell, as shown in Fig. 1. Note that a pseudo critical point  $J_{3\chi}$  is identified as a bifurcation point. Therefore, a continuous QPT occurs at  $J_3 \sim 1.0001$ .

(iii) The ground-state fidelity per lattice site,  $d(J_2, J'_2)$ , as a function of  $J_2$ , at a fixed  $J'_2$ , is plotted in Fig. 4 for  $J_3 = 1.5$ , with  $J_2$  as the control parameter. In addition, the reference state  $|\varphi(J'_2)\rangle$  is fixed at  $J'_2 = 0.1$ . Spontaneous symmetry breaking of the translation group  $Z_3$  under three-site shifts occurs for  $J_2 > 0$ . There is a jump at  $J_2 = 0$  in the ground-state fidelity per lattice site, meaning that the phase transition is discontinuous. The pseudo critical points are shown for different values of the truncation dimension, without any significant shift, when  $\chi$  is increased from  $\chi = 8$  to  $\chi = 32$ .

*Local order parameters.* In the conventional Ginzburg-Landau-Wilson paradigm, a central concept is local order parameters, whose nonzero values characterize symmetry broken phases. As advocated in Ref. [25], any local order parameter may be derived from a reduced density matrix from a representative ground-state wave function in a symmetry broken phase, if its iMPS representation is known. Actually, this follows from the non-zero-entry structure of a reduced density matrix: in a symmetric phase, any reduced density matrix respects all the symmetry of the system, but in a symmetry broken phase, there are extra nontrivial entries in a reduced density matrix due to the fact that a symmetry operation is lost. Following this line of reasoning, we are able to derive local order parameters for different symmetry broken phases.

In the  $Z_3$  symmetry broken phase, three degenerate ground states arise. The non-zero-entry structure of the one-site reduced density matrix yields a local order parameter  $\mathcal{O}_{M1} = (\langle \sigma_z^A \rangle - 2\langle \sigma_z^B \rangle + \langle \sigma_z^C \rangle)/4$ , which is shown in Fig. 5(a). In fact, we may equally choose any of the following three operators as a local order parameter:  $(-2\langle \sigma_z^A \rangle + \langle \sigma_z^B \rangle + \langle \sigma_z^C \rangle)/4$ ,  $(\langle \sigma_z^A \rangle - 2\langle \sigma_z^B \rangle + \langle \sigma_z^C \rangle)/4$ , and  $(\langle \sigma_z^A \rangle + \langle \sigma_z^B \rangle - 2\langle \sigma_z^C \rangle)/4$ , where  $A, B$ , and  $C$  label three sites in the unit cell, as shown in Fig. 1.

In the  $G$  symmetry broken phase, four degenerate ground states arise. A local order parameter may be constructed from an analysis of the non-zero-entry structure of the one-site reduced density matrix. One may choose  $\langle \sigma_z^A \rangle, \langle \sigma_z^B \rangle$ , and  $\langle \sigma_z^C \rangle$  as a local order parameter, which are able to distinguish four degenerate ground states. Their magnitudes take the same value, which is shown in Fig. 5(b).

Now we take advantage of the finite-entanglement scaling

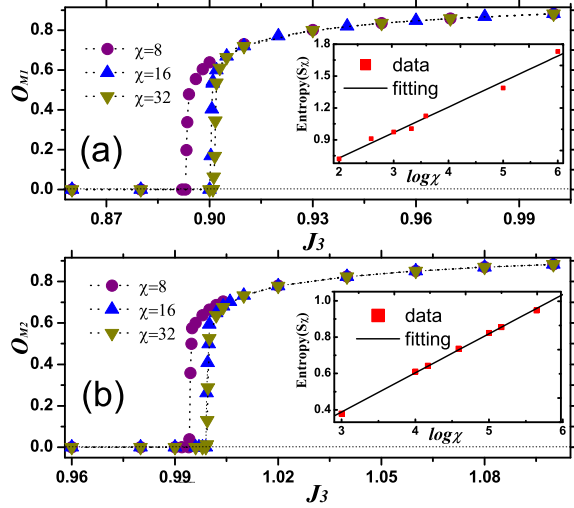


FIG. 5: (color online) Main: The local order parameter  $O_{M1} = (\langle \sigma_z^A \rangle - 2\langle \sigma_z^B \rangle + \langle \sigma_z^C \rangle)/4$  shown in (a) and  $O_{M2} = \langle \sigma_z \rangle$  shown in (b) for a 1D spin model with the competing two-spin and three-spin interactions, where  $J_2 = 0.4$  and  $J_2 = 0$ , respectively. The computation is performed with the truncation dimension  $\chi = 8, 16$  and  $32$ . The pseudo critical points located by the order parameter are consistent with those obtained by the ground-state fidelity per lattice site. We see that  $O_{M1}$  and  $O_{M2}$  tend to saturate, with increasing  $\chi$ . Inset: The extrapolation of the semi-infinite chain von Neumann entropy is performed, yielding the central charge  $c \sim 0.796$ , with respect to the bond dimension  $\chi = 4, 6, 8, 10, 12, 32$  and  $64$ , in (a) and  $c \sim 0.994$ , with respect to the bond dimension  $\chi = 8, 16, 18, 24, 32, 36$  and  $50$ , in (b), very close to the exact results  $c = 4/5$  and  $1$ , respectively.

of the von Neumann entropy to determine the nature of the criticalities. The von Neumann entropy  $S$  for a semi-infinite chain scales as  $S \sim \kappa/6 \log \chi$ , where  $c$  is the central charge, and  $\kappa$  is the finite-entanglement scaling exponent [26]. Our best fitting results, as shown in the insets of Fig. 5 (a) and (b), yields the central charge  $c \sim 4/5$  and  $c \sim 1$ , with  $\kappa \sim 1.8077$  and  $\kappa \sim 1.2996$ , respectively. This implies that the transition points  $J_{3c} \sim 0.9034$  and  $J_{3c} \sim 1.0001$  are, respectively, in the same universality class as the three-state Potts universality class and the four-state Potts universality class.

**Conclusions.** We have investigated a quantum spin model with the competing two-spin and three-spin interactions by exploiting a tensor network algorithm based on the iMPS representation. The algorithm itself is an adaptation of Vidal's iTEBD algorithm to a translation-invariant 1D lattice spin system with three-spin interactions. This enables us to efficiently compute the ground-state fidelity per lattice site, which in turn makes it possible to locate critical points by identifying bifurcation points in the ground-state fidelity per lattice site. For a few selected values of the coupling constants, we succeeded in identifying critical points, and deriving local order parameters to characterize different phases in the conventional Ginzburg-Landau-Wilson paradigm.

**Acknowledgements.** We thank Sam Young Cho, Bo Li,

Sheng-Hao Li, Qian-Qian Shi, Ai-Min Chen, Yao-Heng Su, Jian-Hua Liu and Jian-Hui Zhao for helpful discussions. The work is partially supported by the National Natural Science Foundation of China (Grant No: 10874252). HLW and YWD are supported by the Fundamental Research Funds for the Central Universities (Project No. CDJXS11102214) and by Chongqing University Postgraduates' Science and Innovation Fund (Project No.: 200911C1A0060322).

- 
- [1] S. Sachdev, Quantum Phase Transitions, Cambridge University Press, 1999, Cambridge.
  - [2] X.-G. Wen, Quantum Field Theory of Many-Body Systems, Oxford University Press, 2004, Oxford.
  - [3] A. Bermudez, D. Porras, and M. A. Martin-Delgado, Phys. Rev. A **79**, 060303 (2009).
  - [4] J. K. Pachos and M. B. Plenio, Phys. Rev. Lett. **93**, 056402 (2004).
  - [5] H. P. Büchler, A. Micheli, and P. Zoller, Nat. Phys. **3**, 726 (2007).
  - [6] G. Vidal, Phys. Rev. Lett. **98**, 070201 (2007); G. Vidal, Phys. Rev. Lett. **93**, 040502 (2004); G. Vidal, Phys. Rev. Lett. **91**, 147902 (2003).
  - [7] J. Jordan, R. Orús, G. Vidal, F. Verstraete, and J.I. Cirac, Phys. Rev. Lett. **101**, 250602 (2008).
  - [8] L. Amico, R. Fazio, A. Osterloh, and V. Vedral, Rev. Mod. Phys. **80**, 517 (2008) and references therein.
  - [9] H.-Q. Zhou and J.P. Barjaktarević, J. Phys. A: Math. Theor. **41**, 412001 (2008); H.-Q. Zhou, J.-H. Zhao, and B. Li, J. Phys. A: Math. Theor. **41** (2008) 492002; H.-Q. Zhou, arXiv:0704.2945.
  - [10] H.-Q. Zhou, R. Orús, and G. Vidal, Phys. Rev. Lett. **100**, 080602 (2008).
  - [11] J.-H. Zhao, H.-L. Wang, B. Li, and H.-Q. Zhou, Phys. Rev. E. **82**, 061127 (2010).
  - [12] H.-L. Wang, J.-H. Zhao, B. Li, and H.-Q. Zhou, arXiv: 0902.1670.
  - [13] Y.-W. Dai, B.-Q. Hu, J.-H. Zhao, and H.-Q. Zhou J. Phys. A: Math. Theor. **43**, 372001 (2010).
  - [14] P. Zanardi and N. Paunković, Phys. Rev. E **74**, 031123 (2006).
  - [15] P. Zanardi, M. Cozzini, and P. Giorda, J. Stat. Mech. (2007) L02002; M. Cozzini, R. Ionicioiu, and P. Zanardi, Phys. Rev. B **76** 104420 (2007); L. Campos Venuti and P. Zanardi, Phys. Rev. Lett. **99**, 095701 (2007).
  - [16] N. Oelkers and J. Links, Phys. Rev. B **75**, 115119 (2007).
  - [17] W.-L. You, Y.-W. Li, and S.-J. Gu, Phys. Rev. E **76**, 022101 (2007); S. J. Gu *et al.*, Phys. Rev. B **77**, 245109 (2008).
  - [18] M. F. Yang, Phys. Rev. B **76**, 180403(R) (2007); Y. C. Tzeng and M.F. Yang, Phys. Rev. A **77** 012311 (2008); J. O. Fjærestad, J. Stat. Mech. P07011 (2008); J. Sirker, Phys. Rev. Lett. **105**, 117203 (2010).
  - [19] D. Schwandt, F. Alet, and S. Capponi, Phys. Rev. Lett. **103**, 170501 (2009).
  - [20] R. Orús, T.-C. Wei, and H.-H. Tu, arXiv:1010.5029.
  - [21] V. Mukherjee, A. Polkovnikov, and A. Dutta, Phys. Rev. B **83**, 075118 (2011); V. Mukherjee and A. Dutta, arXiv:1101.1713.
  - [22] M.M. Rams and B. Damski, Phys. Rev. Lett. **106**, 055701 (2011).
  - [23] P.W. Anderson, Basic Notions of Condensed Matter Physics, Addison-Wesley: The Advanced Book Program, 1997, Reading, Mass.

- [24] S. Coleman, An Introduction to Spontaneous Symmetry Break-down and Gauge Fields, Laws of Hadronic Matter, Ed. A. Zichichi, Academic, 1975, New York.
- [25] H.-Q. Zhou, arXiv:0803.0585.
- [26] L. Tagliacozzo L, R. Oliveira Thiago, S. Iblidir, and J.I. Latorre, Phys. Rev. B **78**, 024410 (2008); F. Pollmann, S. Mukerjee, A. Turner, and J.E. Moore, Phys. Rev. Lett. **102**, 255701 (2009).